Chalcogenide Letters Vol. 13, No. 8, August 2016, p. 381 - 388

CHARACTERIZATION OF $CuInSe_2$ THIN FILMS OBTAINED BY RF MAGNETRON CO-SPUTTERING FROM CuSe AND In TARGETS

J.I. MONTES-MONSALVE[a,b*], A. MORALES-ACEVEDO[c],
R. BERNAL-CORREA[d], A. PULZARA-MORA[a]
[a]*Laboratorio de Nanoestructuras Semiconductoras, Universidad Nacional de Colombia, sede Manizales. A.A. 127.*
[b]*Escuela de Materiales, Facultad de Minas, Universidad Nacional de Colombia, sede Medellín.*
[c]*CINVESTAV-IPN, Departamento de Ingeniería Eléctrica, Avenida IPN No. 2508, 07360 Ciudad de México, México.*
[d]*Grupo DEMA, Facultad de Ciencias e Ingeniería, Universidad del Sinú-Elías BecharaZainúm, Montería - Colombia*

The effect of the substrate temperature, from 550° C to 650° C, on the optical and structural properties of $CuInSe_2$ thin films deposited on glass substrates by R.F. Magnetron co-Sputtering of CuSe and In targets was studied. The characterization of the films was carried out via SEM, EDX, XRD, XPS, Raman spectroscopy and optical absorption in the UV-Visible range. SEM images taken in plain view show a change in the films morphology as a function of the experimental parameters, and EDX show films with Cu-poor composition. The influence of the temperature on the crystallite sizes and micro-stress was evaluated by XRD. Finally, the results show that the samples are polycrystalline with the tetragonal chalcopyrite $CuInSe_2$ structure. The Raman measurements revealed the presence of an In_2Se_3 phase in the samples. The UV-Vis optical measurements showed the presence of a $CuInSe_2$ layer with a typical bandgap around 1.1 eV, together with other layers formed by homogeneous mixtures of $CuInSe_2$ + In_2Se_3 with larger effective band-gaps.

(Received July 13, 2016; Accepted August 27, 2016)

Keywords: Characterization, Magnetron Sputtering, Thin films, CIS

1. Introduction

Nowadays, photovoltaic cells development work is focused on the preparation of materials that allow efficient solar energy conversion into electricity, involving growth techniques with low manufacturing costs [1]. In this regard, the chalcopyrite semiconductors such as $CuInSe_2$ (CIS) and $Cu(In,Ga)Se_2$ (CIGS) have become attractive materials to be scaled to industrial production level [2]. Thin film solar cells based on chalcopyrite type materials greatly reduce the material usage since a minimum quantity of material is required for sunlight to be efficiently absorbed. This characteristic is a consequence of the high sunlight absorption coefficient ($\sim 10^5$ cm^{-1}) due to chalcopyrite materials. In addition, chalcopyrite materials have an adequate bandgap and high thermal stability, which have made them adequate as the active layer in solar cells. It is relevant to mention that CIGS and CIS solar cells have already reached maximum conversion efficiencies of 20.8% [3] and 22.3% [4], respectively, in areas of about 0.5 cm^2. CIGS cells are processed through co-evaporation in three stages [3, 5, 6] while for CIS cells the deposition occurs in a two-stage process which includes selenization of the deposited materials. The main disadvantage of the co-evaporation process in three stages lies in its scalability to industrial production level, since it would require relatively long production times

*Corresponding author: jimontesmo@unal.edu.co

and several lines of evaporation sources. Similarly, the two-stage process for CIS solar cells has the disadvantage of an additional selenization and annealing processes [7, 8].

Despite the considerable progress made in terms of industrial scalability, it is necessary to spare no effort in the processes to obtain chalcopyrite type materials such as $CuInSe_2$, and it is imperative to improve deposition techniques such as RF-magnetron sputtering, which has been widely used for making thin film solar cells [9]. Among the known advantages for this technique are: high adhesion to the substrate, ease of material deposition on any type of substrate, high deposition rate and control on the required thickness with a high degree of uniformity [10]. Chalcopyrite $CuInGaSe_2$ has been grown by sequential RF-sputtering for making cells with conversion efficiencies of up to 13.6 %, with the absorbent layer obtained from $(In,Ga)Se_2$ and CuSe targets followed by a subsequent selenization process at 550 °C for 30 min [11]. Additionally, the growth of $CuInSe_2$ from two different targets such as In_2Se_3 and Cu_2Se by RF Magnetron Sputtering with a subsequent heat treatment and selenization has also been reported [12].

In this work, we report the deposition of $CuInSe_2$ by RF magnetron co-sputtering from CuSe and In targets, in order to avoid post-heat treatment and post-selenization processes. However, the deposition conditions have to be optimized to prevent the formation of secondary phases, but it is an alternative for obtaining $CuInSe_2$ in order to reduce one step in the deposition process.

2. Experimental details

The unique step for the thin film deposition was carried out by simultaneous sputtering of CuSe and In targets on glass substrates. Previously to the deposition of the samples, the substrates were cleaned with acetone in an ultrasound bath. CuSe and In commercial targets (with 99.99% purity) with diameters of 2 inches and 1 inch, respectively were used in this process. The background chamber pressure before deposition was $1x10^{-6}$Torr. In order to study the influence of the substrate temperature on the structural, optical and morphological properties of the deposited films, the samples were deposited in an Argon atmosphere for 60 minutes, varying the substrate temperature: 550 °C (M1), 600 °C (M2) and 650 °C (M3), assuming the ternary compound is formed at temperatures above 500 °C [13]. The power used during the deposition was 30 W for CuSe and 15 W for In, respectively. The target-substrate distance was set at 5 cm, and the targets were tilted 35° with respect to the normal of the substrate. The working Ar pressure was kept at $5x10^{-3}$Torr for all the samples. The thickness of the films measured by means of a profilometer were 510 nm (550 °C), 480 nm (600 °C) and 520 nm (650 °C), respectively. To investigate the crystallographic properties of the as-prepared thin films, X-ray diffraction (Panalytical model Xpert pro) 2θ scans were performed in the range from 10 to 100° using the Cu Kα line as the X-ray source. The surface morphology was observed by scanning electron microscopy (SEM). The bandgap (Eg), was determined from optical transmittance measurements at room temperature with non-polarized light at normal incidence in the UV-Visible range with a UV-Visible JASCO's V-670spectrometer. In order to analyze the composition of the films and study possible phases present in the thin films we used both Raman and XPS measurements. Raman spectroscopy measurements were made with a Raman spectrometer Horiba HR800 using a backscattering geometry. Finally, XPS measurements were also made using a Thermo Scientific K-Alpha X-ray Photoelectron Spectrometer (XPS) System.

3. Results and Discussion

The surface morphologies for different growth temperatures were observed via SEM images (10 x 10 μm^2 scan area), as shown in Fig. 1. A clear evidence of the effect of deposition temperature on the film morphologies can be observed. The sample grown at 550 °C is quite dense, with uniform and compact surface, while the samples grown at 600 °C and 650 °C show a laminar morphology with different sizes and shapes.

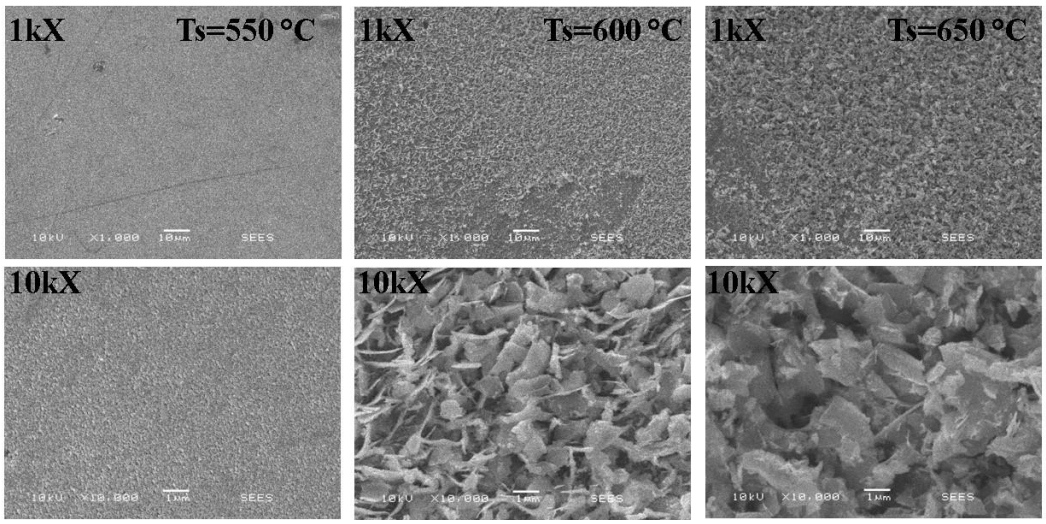

Fig. 1. SEM-Micrographs for the samples deposited at different temperatures at 1 kX and 10 kX magnifications.

The atomic composition analysis was made by EDX measurements and as shown in table 1.

Table 1. Atomic composition of the films grown at different temperatures as determined by EDS.

Sample	Cu (at.%)	In (at.%)	Se (at.%)
550ºC	9.8	30.9	59.1
600ºC	11.8	29.3	58.3
650ºC	6.8	39.4	53.7

This result indicates that the films are poor in Cu and rich in In, showing a composition dependence on the substrate temperature and indicating the possibility of a secondary phase In-rich in the films. Therefore, in order to corroborate the presence of other phases present in the samples, XRD measurements were carried out on the films deposited as a function of the substrate temperature Ts = 550 °C, 600 °C and 650 °C and showed in the Fig. 2.a. It can be seen that the films have a polycrystalline structure with three plane orientations located at 2θ = 26.63°- plane (112), 44.20° - plane (204/220) and 52.35°-plane (116/312). These peaks correspond to the $CuInSe_2$ chalcopyrite tetragonal structure, according to the JCPDS No 089-5649 card. Notice that the peak located at 2θ = 26.63° could also correspond to In_2Se_3 with a hexagonal structure. Additionally, from the X ray diffraction spectra, the micro-stress and the crystallite sizes in the films were estimated by the Williamson-Hall method:

$$FWHM\ x\ cos\theta = \frac{K\,\lambda}{D} + 4\,\varepsilon\ sen\theta \qquad (1)$$

where k is a shape factor ~0.9 for a spherical shape, λ (1.54059 Å) is the wavelength of Cuk_α radiation, D is the crystallite size, FWHM is the effective width of the peak at half-maximum intensity, θ is the diffraction angle at which the peak appears and ε correspond to the micro-stress.

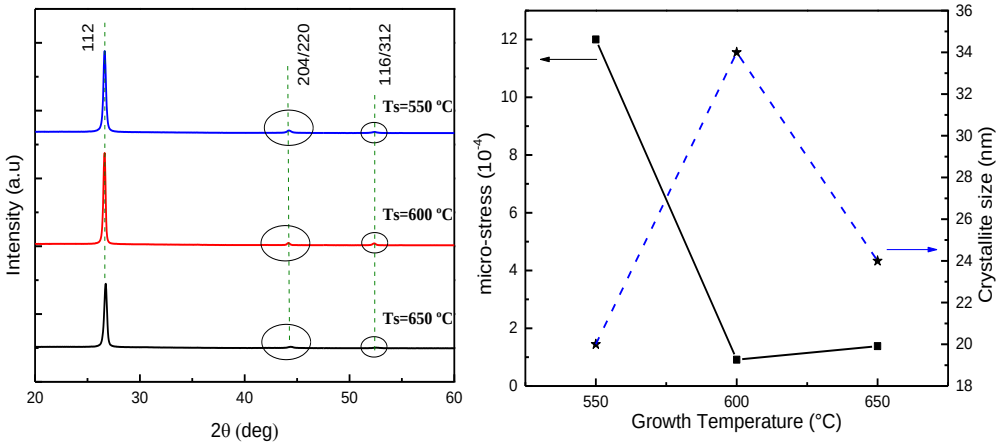

Fig. 2. (a) XRD spectra and (b) micro-stress and crystallite size of the samples grown at 550 °C, 600 °C and 650 °C.

In this method, the micro-stress is assumed uniform throughout the crystallographic directions and is determined by plotting $FWHM\ x\ Cos\theta$ vs $Sen\theta$. The slope of the linear fit leads to the micro-stress value shown in Fig. 2.b as a function of the substrate temperature and the crystallite size D can be determined from the intercept at the y-axis [14]. The average values of D were 20 nm (Ts = 550° C), 34 nm (Ts = 600° C) and 24 nm (Ts = 650° C) taking into account all orientations of the $CuInSe_2$ tetragonal structure. We also observed that as the substrate temperature increased the micro-stress decreased.

The XPS results are depicted in fig. 3 and show the presence of $CuInSe_2$ and likely another phase present associated to In_2Se_3 in the films. Fig. 3a shows the Cu 2p spectra of all samples fitted with a Gaussian-Lorentzian shape. The Cu $2p_{3/2}$ peaks are located at around 932.2 eV which correspond to the binding energy for $CuInSe_2$ [15]. Fig. 3b shows the In 3d spectra of the samples fitted with an asymmetric shape. The In $3d_{5/2}$ peaks position around 444.7 eV for the samples deposited at 550ºC and 600ºC and 444.9 eV for the sample deposited at 650ºC can be attributed both to $CuInSe_2$ or In_2Se_3 materials [15,16]. Finally, the Gaussian-Lorentzian fitting of the Se 3d spectra (Fig. 3c) of all samples show that the Se $3d_{5/2}$ peaks are located at around 54.3 eV. This binding energy is attributed again to $CuInSe_2$ [15] confirming the presence of this material in the films. All the binding energies associated with the elements present in the films are consistent with the values reported in literature [17, 18]. The sample deposited at 650ºC shows also a minor component with the Se $3d_{3/2}$ peak around 55.3 eV that can be attributed to Se-Se bonds [15]. Minor contents of carbon and oxygen were also found in the surface of the samples (spectra not shown here) and can be attributed to adventitious carbon typically found on the surface of thin films exposed to the atmosphere. Furthermore, the relative chemical compositions (in at.%) of the deposited films are listed in Table 2. It is clearly seen that the composition of the films resemble the composition obtained by EDX (table 1).

Table 2. Relative atomic compositions of the samples deposited at different substrate temperatures, as determined by XPS.

Sample	Cu (at.%)	In (at.%)	Se (at.%)
550ºC	8.4	36.7	54.9
600ºC	11.1	33.2	55.7
650ºC	5.7	44.0	50.3

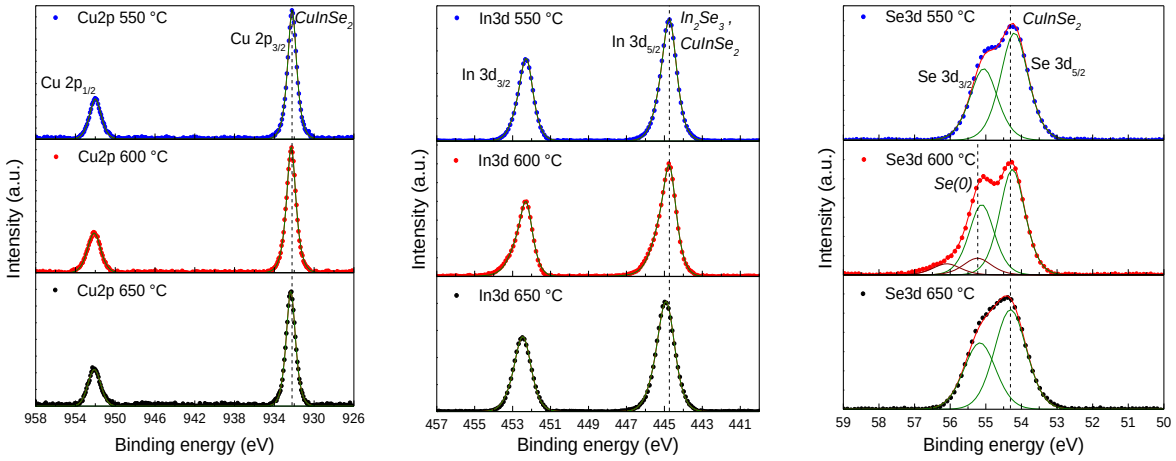

Fig. 3. Fitted XPS Cu 2p, In 3d and Se 3d spectra for the different films.

Study of the samples was also carried out by Raman spectroscopy. This technique is very sensitive to the varying crystalline quality (structural defects, secondary phases and/or micro-stress) of the films deposited on different conditions. Analysis of the vibrational modes in the spectra also gives information regarding the material composition in terms of the formation of ternary compounds [19]. Fig. 4 shows the Raman spectra of the films obtained by varying the substrate temperature. In these spectra, the main vibrational mode A_1 located at 174 cm^{-1} for T_s = 650 °C, 170 cm^{-1} for T_s = 600 °C and 171 cm^{-1} for T_s = 550 °C, is associated with $CuInSe_2$ [20]. Another peak around 128 cm^{-1} corresponds to amorphous In_2Se_3 according to similar results reported in literature [21, 22]. Furthermore, the presence of a peak at 150 cm^{-1} for the film grown at 650 °C is evident, and it is associated to crystalline In_2Se_3 [23], confirming the presence of In_2Se_3 secondary phases in the films in agreement with the results from EDX and XPS measurements.

A significant difference for the effective width of the peak at half-maximum intensity in the main peak such that for T_s = 550° C and T_s = 600° C it is quasi constant (9.5), but for samples grown at Ts = 650 °C the width is almost the double (18.6), showing structural deterioration as the temperature is increased. Indeed, the presence of peaks associated to In_2Se_3 could lead to inclusion of lattice defects and affect the $CuInSe_2$ in the film. This results show that at higher substrate temperature the crystallinity of the $CuInSe_2$ films is reduced due possibly to the In_2Se_3 secondary phases or layers as explained below.

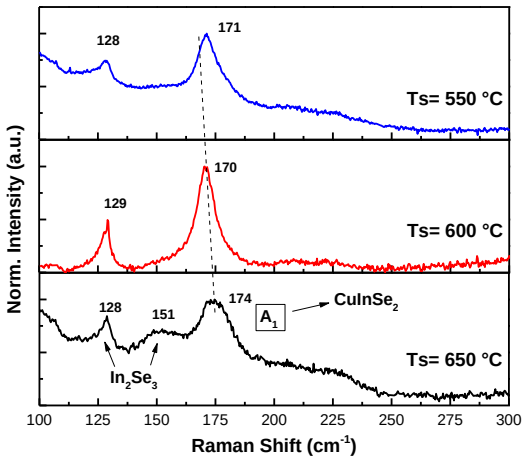

Fig. 4. Raman spectra of the different samples deposited on glass substrates by RF magnetron sputtering.

In order to analyze the optical properties of the deposited films, transmittance measurements were performed in the UV-VIS range. This allowed us to determine the energy bandgap from the square of the product of the absorption coefficient and the photon energy, as a function of energy, as shown in Fig. 5. For the high absorbing region, by plotting $(\alpha h\nu)^2$as a function of photon energy (hν), and extrapolating the linear region of this curve to $(\alpha h\nu)^2 = 0$ we obtain the bandgap value (Eg) for each sample.

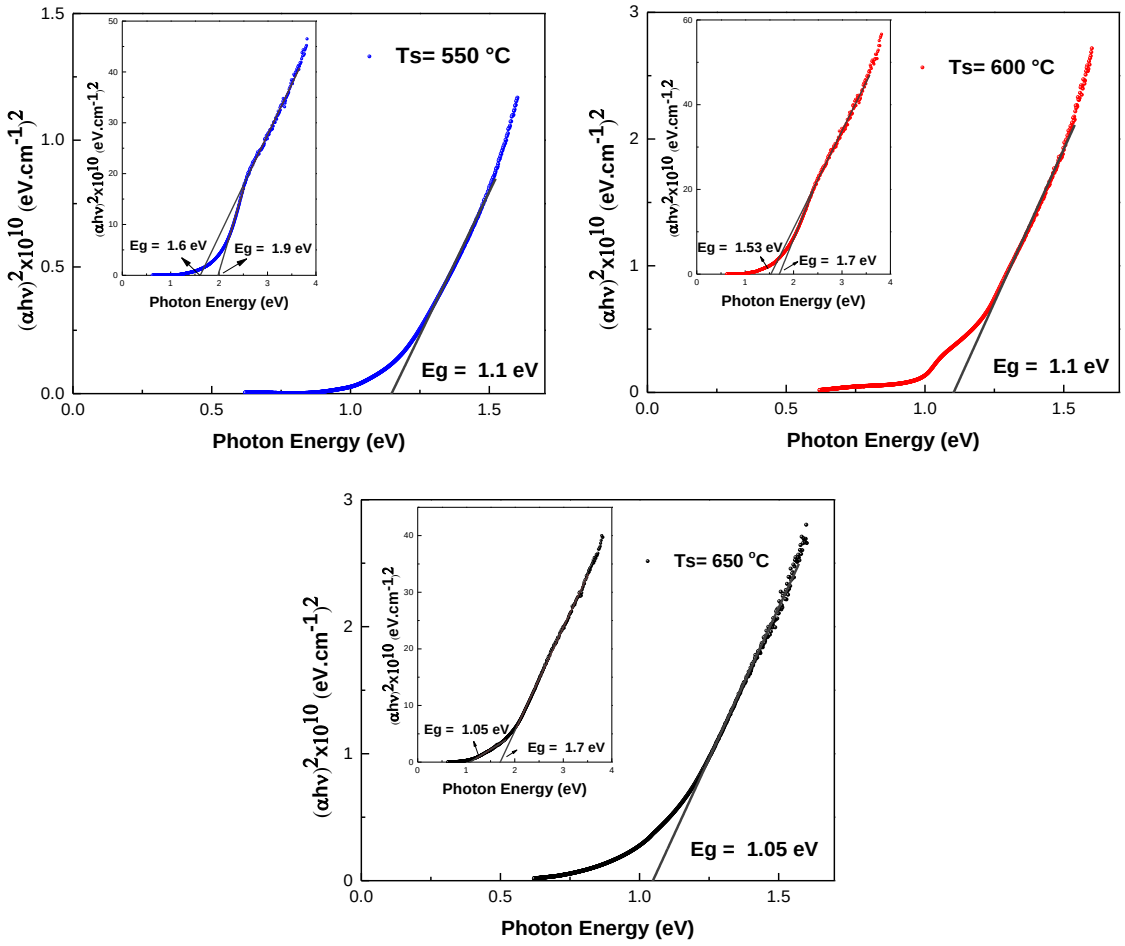

*Fig. 5. Plot of (α*hν)2 vshν for the co-sputtered samples at 550 °C, 600 °C and 650 °C.*

These optical measurements show the presence of at least two direct transitions that demonstrate the existence of at least two layers in the deposited films. For all the films we observe the presence of one layer that can be pure $CuInSe_2$ with bandgap between 1.05 and 1.1 eV, in good agreement with reported values [24] for CIS. However, we also observe the presence of at least one additional layer formed by a homogeneous mixture of $CuInSe_2 + In_2Se_3$. This conclusion is made taking into account the above Raman measurements, which have shown the presence of the In_2Se_3 phases. For the samples grown at low temperatures (550 and 600 °C), two additional layers with different homogeneous mixtures are present. The effective bandgaps for these homogenous mixtures are around 1.6 and 1.9 eV for the samples grown at the lowest temperature (550 °C), while the bandgaps are around 1.5 and 1.7 eV for the samples deposited at 600 °C. For the sample grown at the highest temperature (650°C) there is one layer of $CuInSe_2$ and only one additional layer with a homogeneous mixture of $CuInSe_2 + In_2Se_3$. The bandgap for this layer is around 1.7 eV. These results show that the co-sputtered films are formed by multi-layers with different mixtures of $CuInSe_2$ and In_2Se_3, which has a reported bandgap around 2.1 eV [21]. The different bandgap values indicate different proportions of

In_2Se_3 in the layers. In this regard, the highest deposition temperature is giving only two layers instead of three layers observed for the lower temperatures, but the crystallinity is reduced, as explained above.

In summary, we have shown that RF co-sputtering from CuSe and In targets at substrate temperatures in the range of 550º C to 650º C give multi-layered films with different compositions. One of the layers is polycrystalline $CuInSe_2$, with a bandgap around 1.05-1.1 eV, while the other layers are homogeneous $CuInSe_2$ + In_2Se_3 mixtures with larger bandgaps depending upon the In_2Se_3 proportion in the mixtures. These results are all consistent with Raman, XPS and XRD measurements.

4. Conclusion

$CuInSe_2$ thin films were obtained from simultaneous deposition of CuSe and In targets via R.F magnetron sputtering through unique step deposition. The films have a polycrystalline structure with a mixture of tetragonal $CuInSe_2$ crystallites and In_2Se_3amorphous and crystalline phases. The $CuInSe_2$ average crystallite sizes correspond to 20 nm for 550° C, 34 nm for 600° C and 24 nm for 650° C. The optical absorption measurements showed the presence of at least two layers: one that is formed by pure $CuInSe_2$ (bandgap around 1.1 eV), and another layer formed by a homogeneous $CuInSe_2$ + In_2Se_3 mixture with a higher bandgap. These results show that the deposition temperature is an important parameter to optimize in order to obtain $CuInSe_2$ films using two targets like CuSe and In for solar cells applications.

Acknowledgements

This work was partially supported by DIMA projects 23196 - 21895. We thank to Dr. S. Velázquez for XPS measurements and A. Tavira-Fuentes, G. Casados-Cruz, M. Galván and G. López Fabián of SEES-CINVESTAV-IPN, México, for their technical assistance. J.I. Montes-Monsalve thanks to Alianza del Pacífico for the financial support under the program "Plataforma de movilidad estudiantil y académica de la alianza del pacífico". J.I. Montes-Monsalve thank the financial support for Ph. D. scholarships under the "Francisco Jose de Caldas" program of COLCIENCIAS Conv #528.

References

[1] J. Jean, P. R. Brown, R. L. Jaffe, T. Buonassisi, and V. Bulović, Energy Environ. Sci **8**, 1200 (2015).
[2] M. Powalla, G. Voorwinden, D. Hariskos, P. Jackson and R. Kniese, Thin Solid Films **517**, 2111 (2009).
[3] P. Jackson, D. Hariskos, R. Wuerz, W. Wischmann and M. Powalla, Phys. status solidi - Rapid Res. Lett **8**, 219 (2014).
[4] Solar Frontier Press Release, Solar Frontier Sets Thin-Film PV World Record with 22.3 % CIS Cell," 2015. Online, http://www.solar-frontier.com/eng/news/2015/C051171.html (accesed January 2016)
[5] M. A. Contreras, K. Ramanathan, J. AbuShama, F. Hasoon, D. L. Young, B. Egaas, and R. Noufi, Prog. Photovoltaics Res. Appl **13**, 209 (2005).
[6] G. S. Jung, S. H. Mun, D. Shin, R. B. V. Chalapathy, B. T. Ahn, and H. Kwon, RSC Adv **5**, 7611 (2014).
[7] O. Volobujeva, M. Altosaar, J. Raudoja, E. Mellikov, M. Grossberg, L. Kaupmees, P. Barvinschi, Sol. Energy Mater. Sol. Cells **93**, 11 (2009).
[8] M. V. Yakushev, A. V. Mudryi, V. F. Gremenok, V. B. Zalesski, P. I. Romanov, Y. V. Feofanov, R. W. Martin and R. D. Tomlinson, J. Phys. Chem. Solids

64, 2005 (2003).
[9] K. Kushiya, Y. Tanaka, H. Hakuma, Y. Goushi, S. Kijima, T. Aramoto and Y. Fujiwara, Thin Solid Films **517**, 2108 (2009).
[10] P. J. Kelly and R. D. Arnell, Vaccum **56**, 159 (2000).
[11] X. L. Zhu, Y. M. Wang, Z. Zhou, a. M. Li, L. Zhang, and F. Q. Huang, Sol. Energy Mater. Sol. Cells,**113**,140 (2013).
[12] J. Koo, C.-W. Kim, C. Jeong, and W. K. Kim, Thin Solid Films, **582**, 79 (2015).
[13] B. J. Stanbery, Crit. Rev. Solid State Mater. Sci, **27**, 73 (2002).
[14] G. K. Williamson and W. H. Hall, Acta Metall,**1**, 22 (1953).
[15] J. F. Moulder, W. F. Stickle, P. E. Sobol and K. D. Bomben, Handbool of X-ray Photoelectron Spectroscopy, Physical Electronics Inc, (1995).
[16] S. R. Suryawanshi, P. K. Bankar, M. A. More, and D. J. Late, RSC Adv, **5**, 65274 (2015).
[17] D. Cahen, P. J. Ireland, L. L. Kazmerski and F. A. Thiel, J. Appl. Phys,**57**, 4761 (1985).
[18] S. Kohiki, M. Nishitani, T. Negami and T. Wada, Phys. Rev. B, **45**, 9163 (1992).
[19] V. Izquierdo-Roca, X. Fontané, et. al, Thin Solid Films, **517**, 2163 (2009).
[20] H. B. Xie, W. F. Liu, X. Y. Li, F. Yan, G. S. Jiang, and C. F. Zhu, J. Mater. Sci. Mater. Electron, **24**, 475–482 (2013).
[21] C.Hing-Hwa Ho, Sci. Rep,**4**, 1–8 (2014).
[22] I. W. and T. Yamamoto, Jpn. J. Appl. Phys,**24**, 1282–1287 (1985).
[23] S. Marsillac, A. M. Combot-Marie, J. C. Bernède, and A. Conan, Thin Solid Films **288**, 14 (1996).
[24] H. A. E. Neuman H, Perlt B. , Adul-Hussein N.A.K, Tomlinson R.D, Cryst. Res. Technol, **4**, 469 (1982).